Cardiovascular Research (2012) **93**, 120–129
doi:10.1093/cvr/cvr267

N-terminal domain of soluble epoxide hydrolase negatively regulates the VEGF-mediated activation of endothelial nitric oxide synthase

Hsin-Han Hou[1], Bruce D. Hammock[2], Kou-Hui Su[1], Christophe Morisseau[2], Yu Ru Kou[1], Susumu Imaoka[3], Ami Oguro[3], Song-Kun Shyue[4], Jin-Feng Zhao[1], and Tzong-Shyuan Lee[1,5]*

[1]Institute of Physiology, National Yang-Ming University, Taipei 11221, Taiwan; [2]Department of Entomology and Cancer Center, University of California, Davis, CA 95616, USA; [3]Nanobiotechnology Research Center and Department of Bioscience, School of Science and Technology, Kwansei Gakuin University, Japan; [4]Institute of Biomedical Sciences, Academia Sinica, Taipei, Taiwan; and [5]Graduate Institute of Basic Medical Science, China Medical University, Taichung, Taiwan

Received 8 September 2011; revised 21 September 2011; accepted 7 October 2011; online publish-ahead-of-print 8 November 2011

Aims The mammalian soluble epoxide hydrolase (sEH) has both an epoxide hydrolase and a phosphatase domain. The role of sEH hydrolase activity in the metabolism of epoxyeicosatrienoic acids (EETs) and the activation of endothelial nitric oxide synthase (eNOS) in endothelial cells (ECs) has been well defined. However, far less is known about the role of sEH phosphatase activity in eNOS activation. In the present study, we investigated whether the phosphatase domain of sEH was involved in the eNOS activation in ECs.

Methods and results The level of eNOS phosphorylation in aortas is higher in the sEH knockout ($sEH^{-/-}$) mice than in wild-type mice. In ECs, pharmacological inhibition of sEH phosphatase or overexpressing sEH with an inactive phosphatase domain enhanced vascular endothelial growth factor (VEGF)-induced NO production and eNOS phosphorylation. In contrast, overexpressing the phosphatase domain of sEH prevented the VEGF-mediated NO production and eNOS phosphorylation at Ser617, Ser635, and Ser1179. Additionally, treatment with VEGF induced a c-Src kinase-dependent increase in transient tyrosine phosphorylation of sEH and the formation of a sEH–eNOS complex, which was abolished by treatment with a c-Src kinase inhibitor, PP1, or the c-Src dominant-negative mutant K298M. We also demonstrated that the phosphatase domain of sEH played a key role in VEGF-induced angiogenesis by detecting the tube formation in ECs and neovascularization in Matrigel plugs in mice.

Conclusion In addition to epoxide hydrolase activity, phosphatase activity of sEH plays a pivotal role in the regulation of eNOS activity and NO-mediated EC functions.

Keywords Soluble epoxide hydrolase • Endothelial nitric oxide synthase • Phosphatase • c-Src kinase • Angiogenesis

1. Introduction

Soluble epoxide hydrolase (sEH), an enzyme with C-terminal epoxide hydrolase (EH) and N-terminal lipid phosphatase (PT) activities, is widely distributed in mammalian tissues, including arteries, heart, liver, intestine, kidney, brain, and lung.[1,2] A role of the hydrolase activity of sEH in the metabolism of epoxyeicosatrienoic acids (EETs), inflammation, and hypertension is well documented.[3–5] Pharmacological inhibition of hydrolase activity of sEH or genetic deletion of sEH increases the accumulation of EETs and other epoxy fatty acids, which attenuate angiotensin II-induced hypertension and cardiac hypertrophy *in vitro* and *in vivo*. Thus, sEH may be a therapeutic target for hypertension.[5,6] In contrast to the EH activity, little is known about the biological role of N-terminal lipid phosphatase activity. The enzyme is thought to prefer phosphates on lipophilic compounds as a substrate.[1,2] However, whether the phosphatase activity of sEH participates in the function of cardiovascular system and its underlying regulatory mechanism is largely unknown.

Endothelium-derived nitric oxide (NO), a key regulator of vascular tone, is mainly controlled by the activity of endothelial NO synthase (eNOS).[7,8] Dysregulation of eNOS in endothelial cells (ECs) has been implicated in the pathogenesis of hypertension.[9,10] The

* Corresponding author. Tel: +886 2 2826 7365; fax: +886 2 2826 4049, Email: tslee@ym.edu.tw

activity of eNOS is tightly regulated by a complex network of kinase- and phosphatase-dependent pathways.[11] For example, treatment with vascular endothelial growth factor (VEGF) increases the phosphoinositide 3-kinase/Akt-dependent phosphorylation of eNOS, thus leading to eNOS activation and NO bioavailability in ECs.[12] In contrast, VEGF also activates protein phosphatase 2A to dephosphorylate eNOS, thereby decreasing its enzymatic activity.[13] Recently, treatment with exogenous EETs was found to cause EC-dependent vasodilation, which implies that the EH activity of sEH may have a potent role in the regulation of eNOS activity.[14]

In this study, we hypothesize that the phosphatase domain of sEH also plays an important role in regulation of eNOS activation. We first investigate the phosphorylation status of eNOS in arteries isolated from wild-type (WT) mice and sEH-knockout ($sEH^{-/-}$) mice and then delineate the effect of EH or phosphatase domain of sEH in VEGF-induced NO production and eNOS phosphorylation. We also explore the molecular mechanisms underlying the phosphatase domain of sEH-mediated regulation of eNOS activation and examine the role of phosphatase activity of sEH in VEGF-induced angiogenesis *in vitro* and *in vivo*.

2. Methods

2.1 Reagents

Rabbit antibody (Ab) for phospho-eNOS at Ser617, Ser635, Ser-1179, and c-Src was from Cell Signaling Technology (Beverly, MA, USA). Rabbit Abs for eNOS, sEH, mouse Abs for phospho-Ser, phospho-Thr, goat Ab for sEH, FITC-conjugated donkey anti-rabbit Ab, and Protein A/G PLUS-Agarose were from Santa Cruz Biotechnology (Santa Cruz, CA, USA). Mouse Ab for phospho-Tyr was from BD Biosciences (San Jose, CA, USA). Mouse Ab for α-tubulin, rabbit anti-HA, FITC-conjugated goat anti-mouse Ab, PP1, DAF-2 DA, Griess reagent, and rhodamine red-conjugated goat-anti-rabbit Ab were from Sigma-Aldrich (St Louis, MO, USA). Rabbit Ab for Flag was from GeneMark (Taipei, Taiwan). Recombinant human VEGF and the ELISA kit for cGMP were from R&D systems (Minneapolis, MN, USA). DAPI was from Boehringer Mannheim Biochemicals (Basel, Germany). The BrdU proliferation assay kit was from Roche (Mannheim, Germany). N-acetyl-S-farnesyl-L-cysteine (AFC) was from Enzo Life Sciences (Plymouth Meeting, PA, USA). 12-(3-Adamantan-1-yl-ureido)-dodecanoic acid (AUDA) was synthesized as described.[15] ECL Cell Attachment Matrix was from Millipore (Bedford, MA, USA). EnzyChrom™ $NADP^+$/NADPH assay kit was from BioAssay Systems (Hayward, CA, USA). Hydroethidine (HE) and 2′,7′-dichlorofluorescin diacetate (DCFH-DA) were from Molecular Probes (Eugene, OR, USA).

2.2 Animals

The investigation conformed to the Guide for the Care and Use of Laboratory Animals published by the US National Institutes of Health (NIH Publication No. 85-23, revised 1996), and all animal experiments were approved by the Animal Care and Utilization Committee of the National Yang-Ming University. Eight-week-old male C57BL/6J WT and $Ephx2^{tm1/Gon2/J}$ ($sEH^{-/-}$) mice on a C57BL/6J background were purchased from Jackson Laboratory (Bar Harbor, ME, USA). $sEH^{-/-}$ mice were backcrossed to C57BL/6J for at least 10 generations. At the end of experiment, mice were euthanized with CO_2 and then aortas were harvested and stored at −80°C.

2.3 Cell culture

Bovine aortic endothelial cells (BAECs) were obtained from Cell Applications (San Diego, CA, USA) and were cultured in Dulbecco's modified Eagle's medium supplemented with 10% foetal bovine serum, 100 unit/mL penicillin, and 100 μg/mL streptomycin (HyClone, Logan, UT, USA) in a humidified 95% air-5% CO_2 incubator at 37°C.

2.4 Plasmid construction

Coding regions for the *sEH* full-length, N-terminal phosphatase domain and C-terminal hydrolase domain were amplified from mouse cDNA by PCR with the primers 5′-TTA CGC GTG CGC TGC GTG TAG CCG-3′ and 5′-GGT CTA GAC TAA ATC TTG GAG GTC ACT G-3′ for the full-length, 5′-TTA CGC GTG CGC TGC GTG TAG CCG-3′ and 5′-GGT CTA GAC TAC CCT GTG ACC TTC TCC A-3′ for the N-terminal phosphatase domain, and 5′-TTA CGC GTG TCA GCC ATG GAT ATG TGA C-3′ and 5′-GGT CTA GAC TAA ATC TTG GAG GTC ACT G-3′ for the C-terminal hydrolase domain. PCR was performed as follows: 2 min at 94°C, then 15 s at 94°C, 30 s at 58°C, and 2 min at 72°C for 35 cycles. Each amplified DNA fragment was cloned into the pGEMT vector (Promega), verified by sequencing, digested with *Mlu*I and *Xba*I, and then cloned into the pCMV5N-Flag vector. The *sEH* cDNA encoding mutation in hydrolase or phosphatase activity was amplified by PCR (2 min at 94°C, then 15 s at 94°C, 30 s at 61°C, and 2 min at 72°C for 35 cycles) from the EH mutant or PT mutant plasmid, respectively, kindly provided by Dr S. Imaoka[16] (Kwansei Gakuin University, Japan), with the primers 5′-TTA CGC GTA TGA CGC TGC GCG CGG-3′ and 5′- GGT CTA GAC TAC ATC TTT GAG ACC ACC G -3′. Both PCR products were digested with *Mlu*I and *Xba*I and cloned into the pCMV5N-Flag vector. The plasmid with the c-Src mutant, K298M, was kindly provided by Dr K.L. Guan (University of Michigan, USA).

2.5 Detection of NO and cGMP assay

Accumulated nitrite (NO_2^-), the stable breakdown product of NO, in culture media, was measured by mixing an equal volume of Griess reagent and then incubating at room temperature for 15 min. The azo dye production was then analysed by the use of a SP-8001 UV/VIS spectrophotometer (Metertech, Taipei, Taiwan) with absorbance set at 540 nm. Sodium nitrite was used as a standard. NO production was also measured by comparing DAF-2 DA (an NO sensitive dye) fluorescence staining by use of a Nikon TE2000-U fluorescence microscope. Intracellular levels of cGMP in ECs were assessed by ELISA kit according to the manufacturer's instructions and normalized to protein content as determined by the Bradford assay.

2.6 Protein extraction and immunoblot analysis

BAECs were lysed by SDS lysis buffer, which contained 1% Triton, 0.1% SDS, 0.2% sodium azide, 0.5% sodium deoxycholate, and proteinase inhibitors [1 mmol/L phenylmethylsulfonyl fluoride (PMSF), 10 μg/mL aprotinin, 1 μg/mL leupeptin]. Lysates were centrifuged at 12 000 rpm for 5 min, and the resulting supernatant was collected. The extracted protein was quantified by protein assay. Aliquots (50 μg) of cellular lysate was separated by 8% SDS–PAGE and transferred to BioTrace™ PVDF membrane (Pall). After a blocking with 5% skim milk, blots were incubated with primary Abs and then corresponding secondary Abs. The protein bands were detected by use of an enhanced chemiluminescence kit and quantified by use of ImageQuant 5.2 (Healthcare Bio-Sciences, Philadelphia, PA, USA).

2.7 Immunoprecipitation (IP)

Cells were lysed with the immunoprecipitation (IP) lysis buffer, which contained 50 mmol/L Tris (pH 7.5), 5 mmol/L EDTA, 300 mmol/L NaCl, 1% Triton X-100, 1 mmol/L PMSF, 10 μg/mL aprotinin, 1 μg/mL leupeptin, Tyr phosphatase cocktail I, and Ser/Thr phosphatase cocktail II. Cells were sheared by brief sonication on ice, and cellular debris was

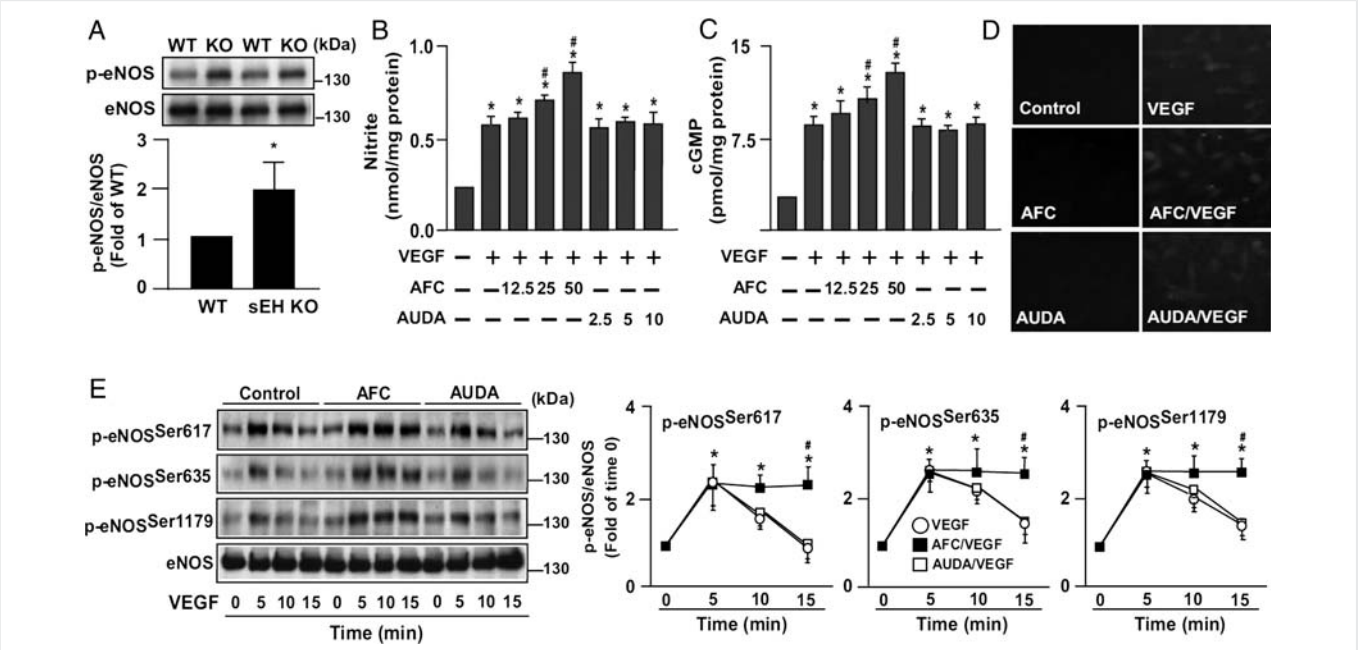

Figure 1 Effect of phosphatase activity or hydrolase activity of sEH in VEGF-induced NO production and eNOS phosphorylation. (*A*) The level of eNOS phosphorylation in aortas from WT or sEH knockout ($sEH^{-/-}$) mice was determined by western blot analysis. (*B* and *C*) BAECs were pre-treated with or without N-acetyl-S-farnesyl-L-cysteine (AFC, an inhibitor of phosphatase activity of sEH, 12.5, 25, 50 μmol/L) or 12-(3-adamantan-1-yl-ureido)-dodecanoic acid (AUDA, an inhibitor of hydrolase activity of sEH, 2.5, 5, 10 μmol/L) for 2 h, then VEGF (50 ng/mL) for 24 h (B and C) or 0–15 min (D and E). Level of nitrite in culture media was measured by Griess assay (*B*). Intracellular content of cGMP was evaluated by the ELISA kit (*C*). DAF-2 DA fluorescence staining was performed to detect NO production (*D*). Cellular lysates were subjected to western blot analysis with Abs for phosphorylated eNOS (p-eNOS) at Ser617, Ser635, and Ser1179 and eNOS (E). $^{*}P < 0.05$ vs. WT mice (*A*) or vehicle-treated cells (*B* and *C*), $^{\#}P < 0.05$ vs. VEGF-treated alone cells (*B*, *C*, and *E*).

removed by centrifugation at 10 000*g* for 10 min. Aliquots (1000 μg) of lysates were incubated with anti-sEH Ab or anti-Flag Ab overnight at 4°C, and then for 2 h at 4°C with 20 μL Protein A/G PLUS-Agarose. Immune complexes were collected by centrifugation and washed three times with ice-cold phosphate-buffered saline (PBS). After a final wash, the supernatant was discarded and the pellet was resuspended in SDS lysis buffer, and then boiled in 5× SDS loading dye for 5 min. Protein was separated by SDS–PAGE and transferred on PVDF membranes. Immunoprecipitated proteins were then detected with anti-HA, anti-Flag, anti-eNOS, anti-phospho-Tyr, or anti-phospho-Ser/Thr Abs.

2.8 Mammalian two-hybrid system

Mouse full-length *sEH* cDNA was sub-cloned into pM vector (Clontech, CA, USA) with the *Mlu*I and *Xba*I cutting site. Human eNOS cDNA was sub-cloned into pVP16 vector (Clontech, CA, USA) with the *Hin*dIII cutting site. Plasmids for control, pM-AD-sEH, pVP16BD-eNOS, and pG5SEAP (secreted human alkaline phosphatase) were co-transfected into BAECs by Lipofectamine 2000. After 48 h, cells were treated with or without VEGF (12.5, 25, and 50 ng/mL) for additional 4 h. Culture media were collected and subjected to chemiluminescence assays by the use of GreatEscAPe SEAP chemiluminescence detection kits (Clontech, CA, USA).

2.9 Confocal microscopy

BAECs were fixed with 4% paraformaldehyde and incubated with 1% bovine serum albumin in PBS. After washing, cells were incubated in mouse anti-eNOS, rabbit anti-sEH, or control Abs at 4°C overnight. After a washing with PBS for three times, cells were incubated with Rhodamine red-conjugated goat anti-rabbit or FITC-conjugated goat-anti-mouse secondary Ab. Images were viewed by Olympus FV1000 laser confocal microscopy (Olympus, Tokyo, Japan).

2.10 *In vitro* angiogenesis (tube formation) assay

The tube formation assay was performed as described.[17] ECL Cell Attachment Matrix was added to 24-well plates and polymerized overnight at 37°C. Cells were seeded onto the layer of matrix gel and incubated in the presence of indicated treatments for 4 h. Tube formation was assessed by microscopy and quantified by counting the number of branch points.

2.11 *In vivo* Matrigel plug angiogenesis assay

To induce the formation of new blood vessels *in vivo*, Matrigel (8 mg/mL) was mixed with heparin (50 U/mL), AFC (50 μmol/L), AUDA (10 μmol/L), with or without VEGF (50 ng/mL), and then injected into subcutaneous tissue of mice. At day 7 postinjection, the Matrigel plugs were removed and photographed. The haemoglobin assay was performed after Matrigel plugs were homogenized and incubated with Drabkin's reagent for 30 min at room temperature. The haemoglobin concentration was calculated at 540 nm.

2.12 Measurement of intracellular reactive oxygen species levels

The membrane-permeable probe HE and DCFH-DA (Molecular Probes, Eugene OR, USA) were used to assess intracellular reactive oxygen species (ROS) levels.[18,19] Oxidation of HE by ROS, preferentially by $O_2^{\bullet -}$, forms red fluorescent ethidium, whereas oxidation of DCFH-DA by ROS, particularly by H_2O_2, yields fluorescent DCFH. Briefly, BAECs

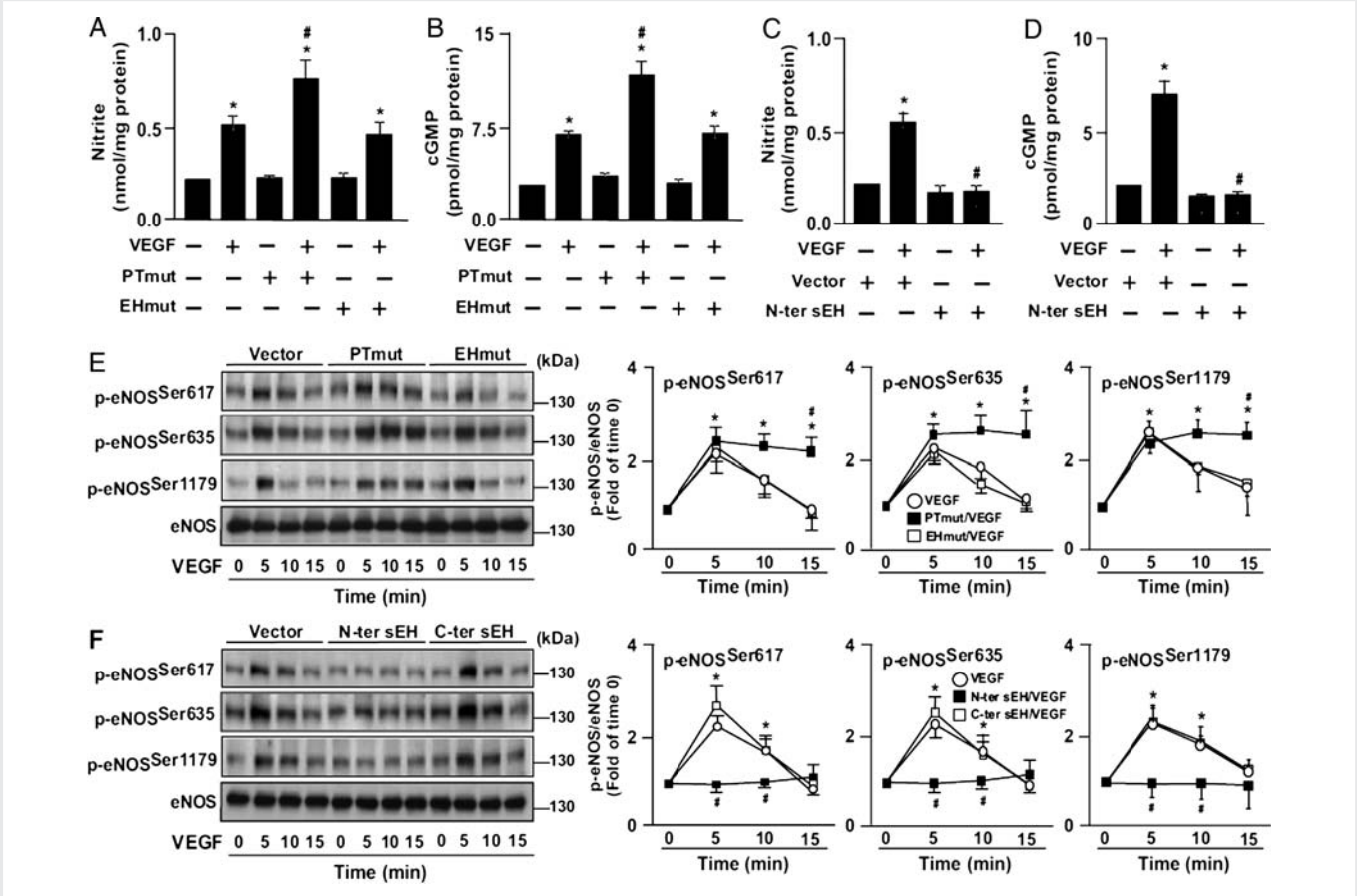

Figure 2 Phosphatase domain of sEH is important for VEGF-induced eNOS phosphorylation and NO production. (*A* and *B*) BAECs were transfected with vector or sEH with mutated phosphatase domain (PTmut) or mutated hydrolase domain (EHmut) for 48 h and then treated with VEGF (50 ng/mL) for 24 h. (*C* and *D*) BAECs were transfected with vector, Flag-tag N-terminal domain of sEH (N-ter sEH) for 48 h and then treated with VEGF (50 ng/mL) for 24 h. Level of nitrite in culture media was measured by the Griess assay. Intracellular content of cGMP was evaluated by the ELISA kit. (*E* and *F*) BAECs were transfected with vector, PTmut, EHmut, N-ter sEH, or C-ter sEH for 48 h and then treated with VEGF for 0–15 min. Cellular lysates were subjected to western blot analysis with Abs for p-eNOS at Ser617, Ser635, and Ser1179 and eNOS. $^{*}P < 0.05$ vs. control, $^{\#}P < 0.05$ vs. VEGF-treated alone group.

were washed with PBS and incubated in cell medium containing 10 μmol/L HE or 20 μmol/L DCFH-DA at 37°C for 45 min. Subsequently, the cell medium containing HE or DCFH-DA was removed and replaced with fresh medium. Cells were then incubated VEGF (50 ng/mL) in the absence or presence of AFC (50 μmol/L) for 30 min. Cells were washed twice with PBS, detached with trypsin/EDTA, and the fluorescence intensity of the cells analysed using an FACScan flow cytometer (Becton Dickinson, San Jose, CA, USA) at 530 nm excitation and 620 nm emission for ethidium and at 488 nm excitation and 530 nm emission for DCF.

2.13 Determination of NADPH oxidase activity

BAECs were incubated VEGF (50 ng/mL) in the absence or presence of AFC (50 μmol/L) for 30 min. The activity of NADPH oxidase was analysed by EnzyChrom™ $NADP^+$/NADPH assay kit according to the manufacturer's instructions.

2.14 Statistical analysis

Results are presented as mean ± SEM from five independent experiments. The Mann–Whitney test was used to compare two independent groups. The Kruskal–Wallis analysis followed by Bonferroni *post hoc* correction was used to account for multiple testing. Statistical analysis involved use of SPSS v8.0 (SPSS Inc., Chicago, IL, USA). A $P < 0.05$ was considered statistically significant.

3. Results

3.1 Phosphatase domain of sEH negatively regulates VEGF-induced NO production and eNOS phosphorylation

We first investigated the role of sEH in regulation of eNOS activation. As revealed by western blot analysis, eNOS phosphorylation in aortas was significantly increased in $sEH^{-/-}$ mice when compared with WT mice (*Figure 1A*). To evaluate the specific role of phosphatase and hydrolase activities of sEH in eNOS activation, BAECs were pre-treated with AFC (an inhibitor of sEH phosphatase activity) or AUDA (an inhibitor of hydrolase activity of sEH).[20] As shown in *Figure 1B–E*, treatment with AFC promoted the VEGF-induced increase in the NO bioavailability and cGMP production. However, AUDA treatment failed to produce such effects. It has been reported that phosphorylation of Ser617, Ser635,

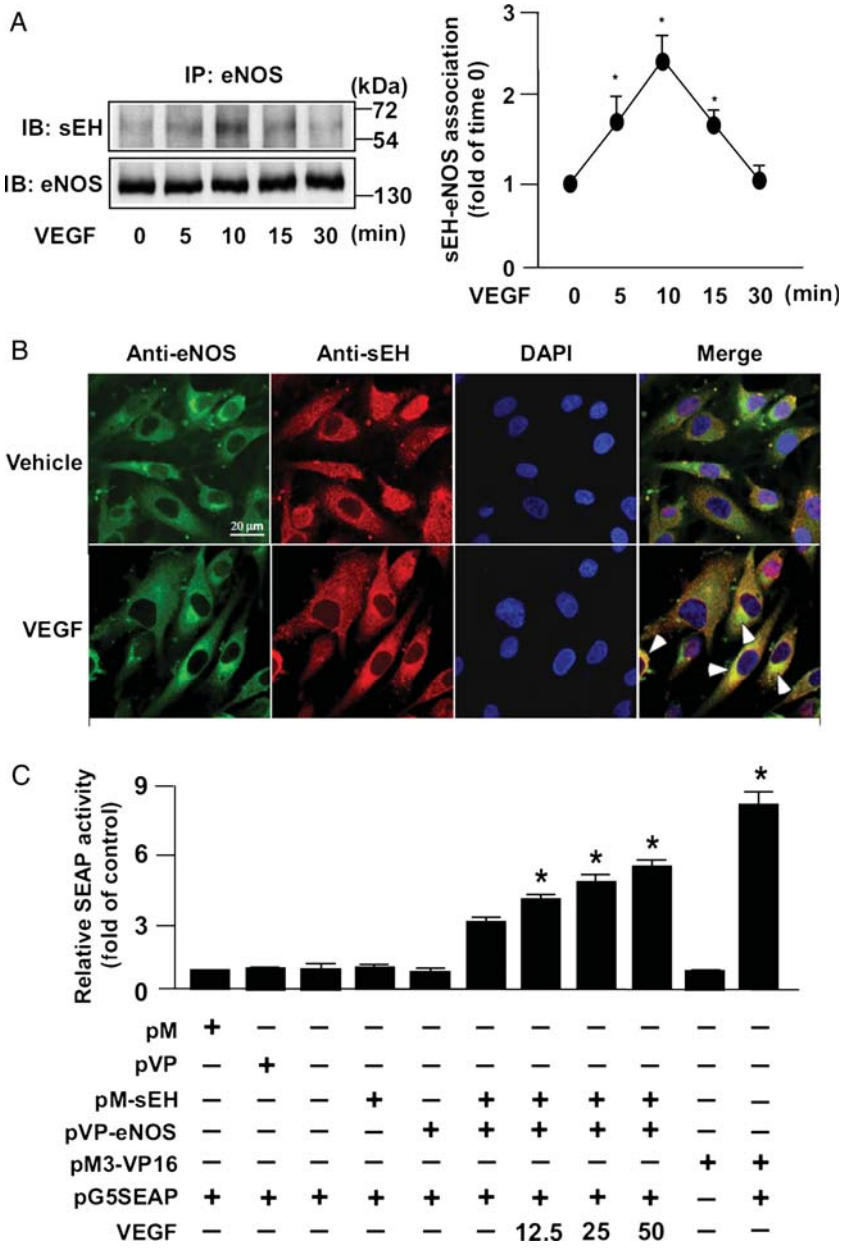

Figure 3 VEGF increases the association of sEH and eNOS. (A) BAECs were treated with VEGF (50 ng/mL) for indicated times. (*A*) Cellular lysates were IP with anti-eNOS Ab and immunoblotted (IB) with anti-eNOS or anti-sEH Ab. (*B*) BAECs were treated with VEGF (50 ng/mL) for 10 min. Cells were then fixed and subjected to immunofluorescence staining with anti-eNOS or anti-sEH Ab. Nuclei were stained with DAPI. The peri-nucleus co-localization of eNOS and sEH was indicated by arrow heads. (*C*) BAECs were cotransfected with pM, pVP, pM-sEH, pVP-eNOS, pM3-VP16, or pG5SEAP for 48 h. Cells were then treated with or without VEGF (12.5, 25, 50 ng/mL) for another 4 h. The pM3-VP16/pG5SEAP-transfected group was as a positive control. The SEAP activity in culture media was determined by GreatEscAPe SEAP chemiluminescence detection kits. *$P < 0.05$ vs. 0 min group (*A*), pM-sEH/pVP-eNOS/pG5SEAP or pM3-VP16 alone group (*C*).

Ser1179, or Thr497 in eNOS plays an important role in the regulation of its enzymatic activity in BAECs.[11] Our data further demonstrated that treatment with AFC prolonged the VEGF-mediated eNOS phosphorylation at Ser617, Ser635, and Ser1179, but had no effect on the eNOS phosphorylation at Thr497 (data not shown). To provide further evidence that phosphatase activity of sEH is critical in eNOS activation, we depleted the phosphatase activity of sEH by overexpressing a full-length sEH with catalytic inactive phosphatase. As shown in *Figure 2A, B, E* and Supplementary material online, *Figure S1*, VEGF-mediated production of NO and cGMP and eNOS phosphorylation at Ser617, Ser635, and Ser1179 were further augmented with overexpression of the inactive phosphatase domain, whereas overexpression of inactive EH domain had no effect. In contrast, overexpression of the phosphatase domain (N-terminus) of sEH totally abrogated VEGF-induced increase in the production of NO and cGMP and eNOS phosphorylation at Ser617, Ser635, and Ser1179 (*Figure 2C, D, F* and Supplementary material online, *Figure S1*). These results indicate that the phosphatase domain of sEH is important in the regulation of eNOS activation.

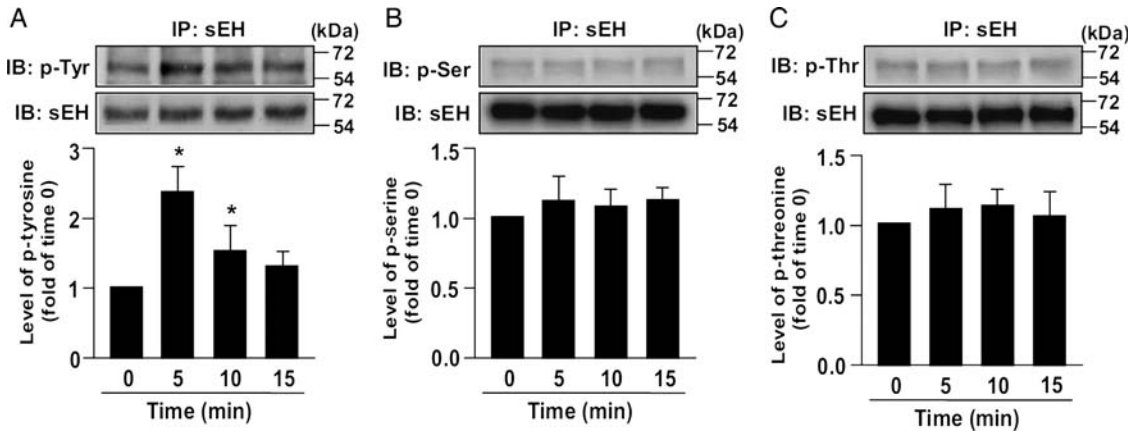

Figure 4 VEGF induces Tyr phosphorylation of sEH. BAECs were treated with VEGF (50 ng/mL) for 0–15 min. Cellular lysates were IP with anti-sEH Ab and IB with anti-Tyr phosphorylation (*A*), anti-Ser phosphorylation (*B*), anti-Thr phosphorylation (*C*), or anti-sEH Abs. $^{*}P < 0.05$ vs. 0 min group.

3.2 VEGF increases the association of sEH and eNOS and tyrosine phosphorylation of sEH

The physiological interaction of eNOS with intracellular proteins plays an important role in the regulation of eNOS activity.[21–23] However, whether sEH interacts directly with eNOS or participates in VEGF-mediated eNOS activation remains unknown. Results from IP assay revealed that sEH was associated with eNOS under normal conditions, and VEGF treatment increased the interaction of sEH and eNOS in a time-dependent manner, with maximal effect at 10 min after treatment (*Figure 3A*). Additionally, the results of confocal microscopy showed that the co-localization of sEH and eNOS was increased in response to VEGF (*Figure 3B*). Additionally, the physical interaction between sEH and eNOS was further supported by the mammalian two-hybrid system. Treatment with VEGF induced an increase in the interaction of pM-sEH and pVP-eNOS, as revealed by the increase in SEAP activity in the medium (*Figure 3C*), which suggests the importance of sEH in eNOS activation. We also found that treatment with VEGF induced a transient tyrosine (Tyr) phosphorylation of sEH within 5–10 min after treatment, which returned to the basal level at 15 min (*Figure 4A*). In contrast, VEGF had no effect on Serine or Threonine phosphorylation of sEH (*Figure 4B* and *C*).

3.3 c-Src signalling is essential for the VEGF-induced increase in sEH phosphorylation and association of sEH and eNOS

In silico modelling (NetPhos 2.0 and NetPhosK 1.0; http://www.cbs.dtu.dk/services/NetPhos/)[24] predicted that c-Src kinase is a possible candidate and may participate in the Tyr phosphorylation of sEH. In addition, c-Src kinase is known to play a key role in VEGF-mediated eNOS activation.[25] Therefore, we examined whether VEGF-induced formation of a sEH–eNOS complex requires Tyr phosphorylation of sEH by c-Src. Pretreatment with PP1 (a c-Src kinase inhibitor) or overexpression with K298M (a c-Src kinase dominant-negative mutant) abolished the VEGF-induced increase in sEH phosphorylation (*Figure 5A* and *B*) and interaction of sEH and eNOS (*Figure 5C* and *D*). Moreover, results of the mammalian two-hybrid system further demonstrated that suppression of c-Src activation inhibited the sEH–eNOS interaction-mediated increase in SEAP activity (*Figure 5E*). These results indicate that c-Src kinase activation is involved in the VEGF-induced increase in sEH phosphorylation and association of the sEH–eNOS complex.

3.4 Phosphatase domain of sEH regulates VEGF-induced angiogenesis

NO-dependent angiogenesis is a critical remodelling process in the development of new blood vessels or in wound healing.[26–29] We next investigated whether the phosphatase domain of sEH is involved in these physiological functions in ECs treated with VEGF. As shown in *Figure 6A*, blocking the phosphatase activity of sEH with AFC or the PT mutant markedly attenuated the VEGF-elicited EC tube formation, as seen by increased number of branch points, whereas AUDA had no effect, which suggests the crucial role of phosphatase activity of sEH in VEGF-mediated promotion of EC tube formation. On the other hand, it has been reported that ROS derived from NAD(P)H oxidase also play a critical role in the regulation of VEGF-mediated angiogenesis.[30] We therefore investigated whether the activity of sEH phosphatase is involved in the VEGF-mediated activation of NAD(P)H oxidase signalling pathway. A shown in Supplementary material online, *Figure S2*, pharmacological inhibition of sEH phosphatase by AFC did not affect VEGF-induced increase in NAD(P)H oxidase activity and ROS production. To confirm the *in vitro* findings, we next used Matrigel plug assay to assess the role of sEH on angiogenesis *in vivo*. As shown in *Figure 6B*, VEGF promoted vascularization, as determined by the haemoglobin content, in Matrigel plugs in WT mice. AFC alone in Matrigel plugs could significantly increase the content of haemoglobin when compared with the control. Moreover, AFC markedly enhanced the VEGF-induced increase in haemoglobin content in Matrigel plugs; however, AUDA failed to generate such effects. Interestingly, the vascularization was greatly augmented in $sEH^{-/-}$ mice with or without VEGF treatment when compared with WT mice.

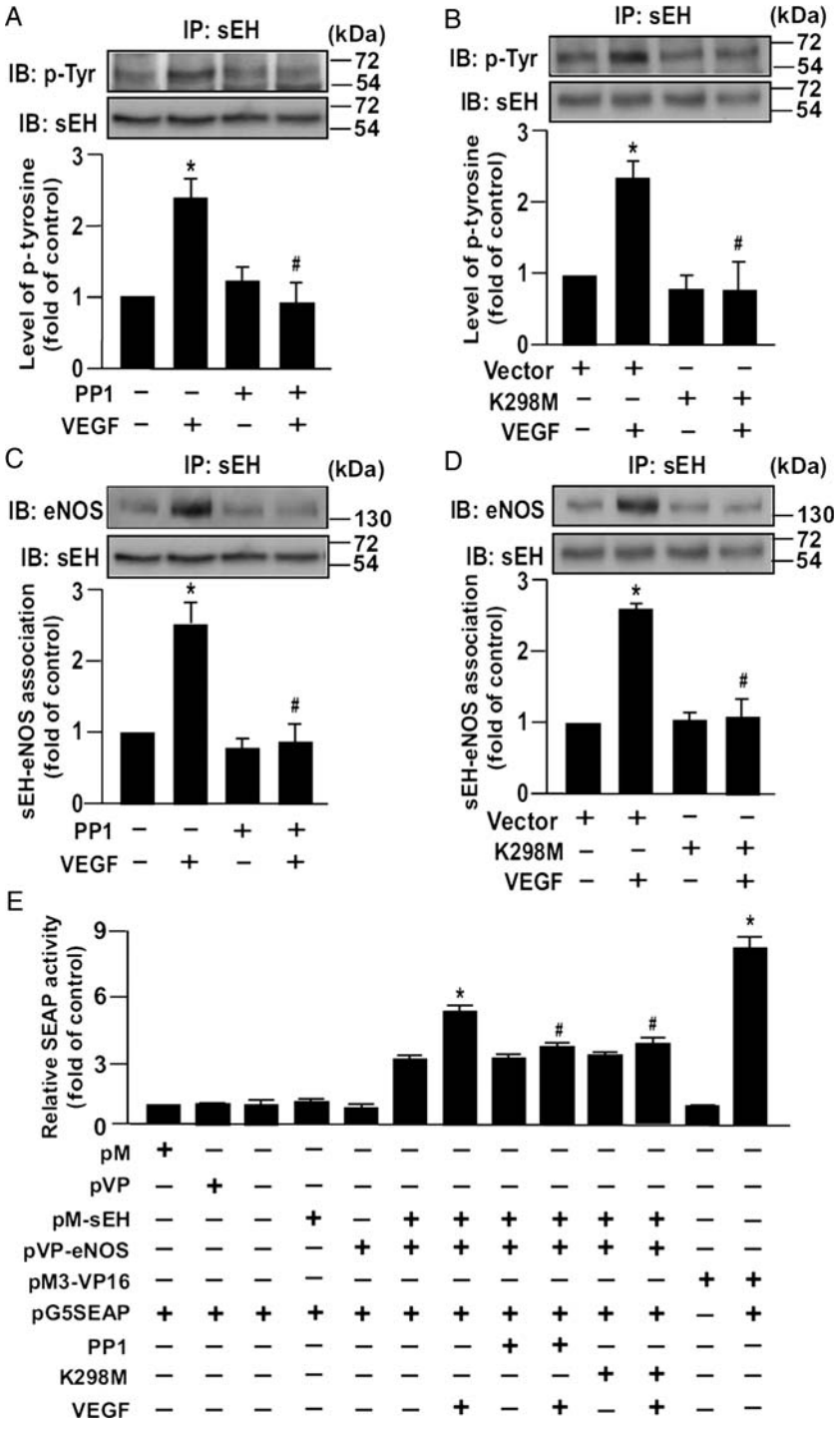

Figure 5 c-Src kinase is required for the VEGF-induced Tyr phosphorylation of sEH and association of sEH and eNOS. BAECs were pretreated with or without PP1 (10 μmol/L, a c-Src inhibitor) for 2 h (*A* and *C*) or were transfected with vector or K298M (a c-Src dominant-negative mutant) for 48 h (*B* and *D*), and then incubated with VEGF (50 ng/mL) for 5 min. Cellular lysates were IP with anti-sEH Ab and then IB with anti-Tyr phosphorylation (*A* and *B*) or anti-eNOS (*C* and *D*) and anti-sEH Abs. (*E*) BAECs were cotransfected with pM, pVP, pM-sEH, pVP-eNOS, pM3-VP16, pG5SEAP, or K298M for 48 h, followed by treatment with or without VEGF (50 ng/mL) or PP1 (10 μmol/L) for another 4 h. The pM3-VP16/pG5SEAP-transfected group was as a positive control. The SEAP activity in culture media was determined by GreatEscAPe SEAP chemiluminescence detection kits. $^{*}P < 0.05$ vs. control (*A*–*D*) or pM-sEH/pVP-eNOS/pG5SEAP transfected group (*E*), $^{\#}P < 0.05$ vs. VEGF-treated alone (*A*–*D*), pM-sEH/pVP-eNOS/pG5SEAP/VEGF or pM3-VP16 alone group (*E*).

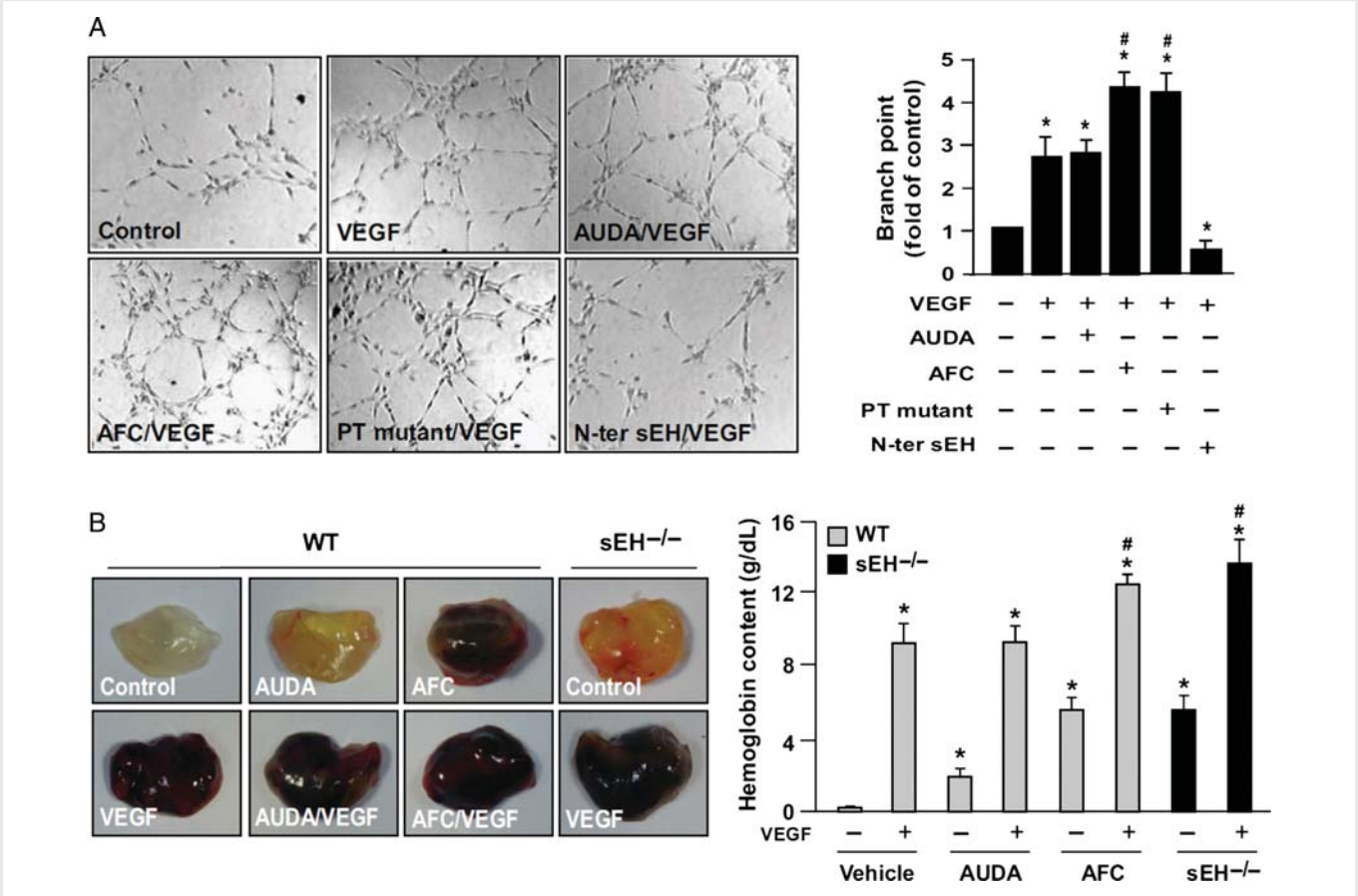

Figure 6 Phosphatase activity of sEH is critical in VEGF-induced angiogenesis *in vitro* and *in vivo*. (*A*) BAECs were pretreated with AFC (50 μmol/L) or AUDA (10 μmol/L) for 2 h or transfected with vector, Flag-tagged sEH with PT mutant domain, and Flag-tagged N-terminal phosphatase domain of sEH (N-ter sEH) for 48 h, then VEGF (50 ng/mL) for 24 h. BAECs were cultured in pre-coated ECL Cell Attachment Matrix in the indicated treatments. Tube formation was visualized, and the bar graphs indicate the fold of branch points in five randomly selected microscopy views. (*B*) Eight-week-old WT mice were subcutaneously injected with Matrigel plugs with or without AFC (50 μmol/L), AUDA (10 μmol/L), VEGF (50 ng/mL), AUDA+VEGF, or AFC+VEGF. $sEH^{-/-}$ mice were subcutaneously injected with Matrigel plugs with or without VEGF (50 ng/mL). At 7 days post-administration, plugs were removed and photographed, and haemoglobin content was analysed. Data are mean ± SEM from 10 mice. $^{*}P < 0.05$ vs. control group, $^{\#}P < 0.05$ vs. VEGF-treated alone WT mice.

These findings suggest that both phosphatase and sEH activities of sEH play a vital role in the physiological function of ECs *in vivo*.

4. Discussion

In this study, we characterized the molecular mechanisms underlying the role of sEH phosphatase activity in the activation of eNOS in ECs. Exposing ECs to VEGF promoted NO production, which was a consequence of increased eNOS phosphorylation.[12] Moreover, we showed that the phosphatase activity of sEH was involved in the regulation of eNOS activity *in vitro* and *in vivo*. Use of pharmacological inhibitors or genetic manipulation revealed that the VEGF-induced eNOS activation was negatively regulated by the phosphatase domain of sEH. We have not addressed if the increased eNOS phosphorylation resulting from inhibition of the phosphatase activity of sEH is a direct or indirect effect on eNOS. In parallel to eNOS activation, exposing ECs to VEGF for only 10 min enhanced the Tyr phosphorylation of sEH and markedly increased the physical interaction of sEH with eNOS. More importantly, this increased sEH–eNOS interaction was abrogated by a specific c-Src kinase antagonist or mutant, which targeted the c-Src signalling pathway. Likewise, the enhanced phosphorylation of sEH and eNOS was prevented by inhibiting the c-Src pathway. Therefore, the c-Src signalling-mediated phosphorylation of sEH and eNOS was required for promoting the formation of the sEH–eNOS complex in ECs stimulated with VEGF. Additionally, we investigated the effect of phosphatase activity of sEH on the activation of eNOS induced by simvastatin, a clinical lipid- lowing drug that is well known for its role in the regulation of eNOS phosphorylation in ECs.[31] Interestingly, inhibition of sEH phosphatase activity further augmented the simvastatin-induced NO production and prolonged the phosphorylation of eNOS (Supplementary material online, *Figure S3*). These findings suggest that the inhibitory effect of sEH phosphatase on eNOS activation was not limited to VEGF stimulation. Collectively, these findings suggest that the phosphatase domain of sEH is vital in the regulation of eNOS activation and physiological function of ECs.

The EH activity of sEH and EETs has been implicated in cardiovascular diseases.[5,6,32–35] For instance, exogenous treatment with EETs cause vessel relaxation through an EC-dependent mechanism.[14] Blockage of the EH activity of sEH by a pharmacological antagonist

significantly attenuated angiotensin II-mediated hypertension[5] and cardiac hypertrophy[6] and retarded the progression of atherosclerosis in experimental animals.[35] Because the N-terminal domain of sEH has been reported to be a phosphatase with isoprenoid mono- and pyrophosphate hydrolysis activity,[36,37] it presumably is a regulator for cellular function. However, the significance of the phosphatase activity of sEH and signalling pathways underlying its regulation of eNOS activity remains elusive. In this study, we targeted the N-terminal phosphatase domain of sEH as a regulator for eNOS activation. We found that the phosphatase activity of sEH is critical for VEGF-mediated eNOS phosphorylation and NO production by using a specific pharmacological inhibitor and plasmids expressing the phosphatase domain of sEH only or full-length sEH with inactive phosphatase.

Our findings regarding the function of the phosphatase activity of sEH are not limited to the cell model. Mixing AFC in a Matrigel plug significantly increased vascularization in the absence or presence of VEGF; AUDA had no such effects, which suggests the critical role of sEH phosphatase activity in EC function. In addition, eNOS phosphorylation in the aortas of $sEH^{-/-}$ mice was increased when compared with the aortas of WT mice. Furthermore, deletion of sEH promoted angiogenesis *in vivo*. However, the vessels of our knockout mice were devoid of both phosphatase and hydrolase domains of sEH, so we cannot determine which domain of sEH contributes to the increase in eNOS phosphorylation and angiogenesis.

Inhibition of EH activity or genetic disruption of sEH in WT mice has resulted in increased concentration of EETs in blood, which indicates the possible involvement of hydrolase activities of sEH in eNOS activation.[38,39] This notion was further supported by results of increased angiogenesis in AUDA-treated WT mice and $sEH^{-/-}$ mice without VEGF treatment. Interestingly, inhibition of the N-terminal phosphatase activity and the C-terminal EH activity should have opposite effects on the regulation of eNOS activity. However, our data suggest that in concert with EETs, the phosphatase activity of sEH in ECs may also participate in the regulation of eNOS activity *in vivo*.

In addition to the phosphorylation- and dephosphorylation-dependent regulation of eNOS activity, the physical interaction of eNOS with intracellular proteins is crucial in the regulation of eNOS activation in response to various stimuli.[11,13,21–23] For example, statins induce the recruitment of heat shock protein 90 to eNOS and facilitates the dissociation of eNOS from caveolin-1, thus leading to eNOS activation.[21] In this study, we showed that sEH associates with eNOS in ECs without stimulation, which is markedly increased in response to VEGF treatment, accompanied by an increase in Tyr phosphorylation of sEH. More importantly, we demonstrated that c-Src kinase, a key regulator in eNOS activation by VEGF or other agonists in ECs,[23] is the upstream signalling molecule for the Tyr phosphorylation of sEH and the formation of a sEH–eNOS complex. Although the exact molecular mechanisms underlying the cross-talk among c-Src, sEH, and eNOS remain to be uncovered, our results are the first to indicate that both kinase-dependent regulation and protein–protein interaction are significantly involved in the VEGF-mediated Tyr phosphorylation of sEH and interaction with eNOS, as well as NO biosynthesis.

In summary, we provide evidence that VEGF triggers the activation of c-Src signalling, which leads to enhanced sEH phosphorylation and increased sEH–eNOS interaction. Ultimately, these alterations negatively modulate the eNOS activation and NO production in ECs. The molecular mechanisms revealed in this study may provide important information for novel pharmacological targets for the treatment of eNOS-related cardiovascular diseases.

Supplementary material

Supplementary material is available at *Cardiovascular Research* online.

Acknowledgements

We thank Dr Todd R. Harris for helpful suggestions for the experiments of mammalian two-hybrid system. The authors thank Laura Smales for help with language editing.

Conflict of interest: C.M. and B.D.H. are employees of the University of California which holds patents in the area of epoxide hydrolase inhibitors for human therapy.

Funding

T.-S.L. was supported by the National Health Research Institutes (NHRI-EX100-9608SC), National Science Council (NSC-99-2320-B-010-017-MY3), Ministry of Education, Aim for the Top University Plan VGHUST Joint Research Program, Tsou's Foundation (VGHUST 99-P6-41 and VGHUST 100-G7-4-4), Yen Tjing Ling Medical Foundation (CI-99-15 and CI-100-26), Taiwan. C.M. and B.D.H. were supported by NIEHS RO1 ES002710. B.D.H. is a George and Judy Marcus senior fellow of the American Asthma Foundation, USA.

References

1. Gill SS, Hammock BD. Distribution and properties of a mammalian soluble epoxide hydrase. *Biochem Pharmacol* 1980;**29**:389–395.
2. Enayetallah AE, French RA, Thibodeau MS, Grant DF. Distribution of soluble epoxide hydrolase and of cytochrome P450 2C8, 2C9, and 2J2 in human tissues. *J Histochem Cytochem* 2004;**52**:447–454.
3. Spector AA, Fang X, Snyder GD, Weintraub NL. Epoxyeicosatrienoic acids (EETs): metabolism and biochemical function. *Prog Lipid Res* 2004;**43**:55–90.
4. Inceoglu B, Jinks SL, Ulu A, Hegedus CM, Georgi K, Schmelzer KR *et al*. Soluble epoxide hydrolase and epoxyeicosatrienoic acids modulate two distinct analgesic pathways. *Proc Natl Acad Sci USA* 2008;**105**:18901–18906.
5. Imig JD, Zhao X, Capdevila JH, Morisseau C, Hammock BD. Soluble epoxide hydrolase inhibition lowers arterial blood pressure in angiotensin II hypertension. *Hypertension* 2002;**39**:690–694.
6. Ai D, Pang W, Li N, Xu M, Jones PD, Yang J *et al*. Soluble epoxide hydrolase plays an essential role in angiotensin II-induced cardiac hypertrophy. *Proc Natl Acad Sci USA* 2009;**106**:564–569.
7. Bredt DS, Snyder SH. Nitric oxide: a physiologic messenger molecule. *Annu Rev Biochem* 1994;**63**:175–195.
8. Griffith OW, Stuehr DJ. Nitric oxide synthases: properties and catalytic mechanism. *Annu Rev Physiol* 1995;**57**:707–736.
9. Schulz E, Jansen T, Wenzel P, Daiber A, Münzel T. Nitric oxide, tetrahydrobiopterin, oxidative stress, and endothelial dysfunction in hypertension. *Antioxid Redox Signal* 2008;**10**:1115–1126.
10. Zhao YY, Zhao YD, Mirza MK, Huang JH, Potula HH, Vogel SM *et al*. Persistent eNOS activation secondary to caveolin-1 deficiency induces pulmonary hypertension in mice and humans through PKG nitration. *J Clin Invest* 2009;**119**:2009–2018.
11. Dudzinski DM, Michel T. Life history of eNOS: partners and pathways. *Cardiovasc Res* 2007;**75**:247–260.
12. Youn JY, Wang T, Cai H. An ezrin/calpain/PI3K/AMPK/eNOSs1179 signaling cascade mediating VEGF-dependent endothelial nitric oxide production. *Circ Res* 2009;**104**:50–59.
13. Michell BJ, Chen Zp, Tiganis T, Stapleton D, Katsis F, Power DA *et al*. Coordinated control of endothelial nitric-oxide synthase phosphorylation by protein kinase C and the cAMP-dependent protein kinase. *J Biol Chem* 2001;**276**:17625–17628.
14. Hercule HC, Schunck WH, Gross V, Seringer J, Leung FP, Weldon SM *et al*. Interaction between P450 eicosanoids and nitric oxide in the control of arterial tone in mice. *Arterioscler Thromb Vasc Biol* 2009;**291**:54–60.
15. Oguro A, Sakamoto K, Suzuki S, Imaoka S. Contribution of hydrolase and phosphatase domains in soluble epoxide hydrolase to vascular endothelial growth factor expression and cell growth. *Biol Pharm Bull* 2009;**32**:1962–1967.
16. Morisseau C, Goodrow MH, Newman JW, Wheelock CE, Dowdy DL, Hammock BD. Structural refinement of inhibitors of urea based soluble epoxide hydrolases. *Biochem Pharmacol* 2002;**63**:1599–1608.

17. Zhou RH, Yao M, Lee TS, Zhu Y, Martins-Green M, Shyy JY. Vascular endothelial growth factor activation of sterol regulatory element binding protein: a potential role in angiogenesis. *Circ Res* 2004;**95**:471–478.
18. Liu PL, Chen YL, Chen YH, Lin SJ, Kou YR. Wood smoke extract induces oxidative stress-mediated caspase-independent apoptosis in human lung endothelial cells: role of AIF and EndoG. *Am J Physiol Lung Cell Mol Physiol* 2004;**289**:L739–L749.
19. Lee TS, Liu YJ, Tang GJ, Yien HW, Wu YL, Kou YR. Wood smoke extract promotes both apoptosis and proliferation in rat alveolar epithelial type II cells: the role of oxidative stress and heme oxygenase-1. *Crit Care Med* 2008;**36**:2597–2606.
20. Enayetallah AE, Grant DF. Effects of human soluble epoxide hydrolase polymorphisms on isoprenoid phosphate hydrolysis. *Biochem Biophys Res Commun* 2006;**341**:254–260.
21. Ju H, Zou R, Venema VJ, Venema RC. Direct interaction of endothelial nitric-oxide synthase and caveolin-1 inhibits synthase activity. *J Biol Chem* 1997;**272**:18522–18555.
22. Averna M, Stifanese R, De Tullio R, Passalacqua M, Salamino F, Pontremoli S *et al*. Functional role of HSP90 complexes with endothelial nitric-oxide synthase (eNOS) and calpain on nitric oxide generation in endothelial cells. *J Biol Chem* 2008;**283**: 29069–29076.
23. Su KH, Tsai JY, Kou YR, Chiang AN, Hsiao SH, Wu YL *et al*. Valsartan regulates the interaction of angiotensin II type 1 receptor and endothelial nitric oxide synthase via Src/PI3K/Akt signalling. *Cardiovasc Res* 2009;**82**:468–475.
24. Blom N, Gammeltoft S, Brunak S. Sequence and structure-based prediction of eukaryotic protein phosphorylation sites. *J Mol Biol* 1999;**294**:1351–1362.
25. Duval M, Le Boeuf F, Huot J, Gratton JP. Src-mediated phosphorylation of Hsp90 in response to vascular endothelial growth factor (VEGF) is required for VEGF receptor-2 signaling to endothelial NO synthase. *Mol Biol Cell* 2007;**18**:4659–4668.
26. Wang S, Li X, Parra M, Verdin E, Bassel-Duby R, Olson EN. Control of endothelial cell proliferation and migration by VEGF signaling to histone deacetylase 7. *Proc Natl Acad Sci USA* 2008;**105**:7738–7743.
27. van Nieuw Amerongen GP, Koolwijk P, Versteilen A, van Hinsbergh VW. Involvement of RhoA/Rho kinase signaling in VEGF-induced endothelial cell migration and angiogenesis *in vitro*. *Arterioscler Thromb Vasc Biol* 2003;**23**:211–217.
28. Duda DG, Fukumura D, Jain RK. Role of eNOS in neovascularization: NO for endothelial progenitor cells. *Trends Mol Med* 2004;**10**:143–145.
29. Heck DE, Laskin DL, Gardner CR, Laskin JD. Epidermal growth factor suppresses nitric oxide and hydrogen peroxide production by keratinocytes. Potential role for nitric oxide in the regulation of wound healing. *J Biol Chem* 1992;**267**: 21277–21280.
30. Ushio-Fukai M, Tang Y, Fukai T, Dikalov SI, Ma Y, Fujimoto M *et al*. Novel role of gp91(phox)-containing NAD(P)H oxidase in vascular endothelial growth factor-induced signaling and angiogenesis. *Circ Res* 2002;**91**:1160–1167.
31. Sun W, Lee TS, Zhu M, Gu C, Wang Y, Zhu Y *et al*. Statins activate AMP-activated protein kinase *in vitro* and *in vivo*. *Circulation* 2006;**114**:2655–2662.
32. Sinal CJ, Miyata M, Tohkin M, Nagata K, Bend JR, Gonzalez FJ. Targeted disruption of soluble epoxide hydrolase reveals a role in blood pressure regulation. *J Biol Chem* 2000;**275**:40504–40510.
33. Imig JD. Cardiovascular therapeutic aspects of soluble epoxide hydrolase inhibitors. *Cardiovasc Drug Rev* 2006;**24**:169–188.
34. Jiang JG, Chen RJ, Xiao B, Yang S, Wang JN, Wang Y *et al*. Regulation of endothelial nitric-oxide synthase activity through phosphorylation in response to epoxyeicosatrienoic acids. *Prostaglandins Other Lipid Mediat* 2007;**82**:162–174.
35. Ulu A, Davis BB, Tsai HJ, Kim IH, Morisseau C, Inceoglu B *et al*. Soluble epoxide hydrolase inhibitors reduce the development of atherosclerosis in apolipoprotein E-knockout mouse model. *J Cardiovasc Pharmacol* 2008;**52**:314–323.
36. Cronin A, Mowbray S, Dürk H, Homburg S, Fleming I, Fisslthaler B *et al*. The N-terminal domain of mammalian soluble epoxide hydrolase is a phosphatase. *Proc Natl Acad Sci USA* 2003;**100**:1552–1557.
37. Newman JW, Morisseau C, Harris TR, Hammock BD. The soluble epoxide hydrolase encoded by EPXH2 is a bifunctional enzyme with novel lipid phosphate phosphatase activity. *Proc Natl Acad Sci USA* 2003;**100**:1558–1563.
38. Yu Z, Xu F, Huse LM, Morisseau C, Draper AJ, Newman JW *et al*. Soluble epoxide hydrolase regulates hydrolysis of vasoactive epoxyeicosatrienoic acids. *Circ Res* 2000;**87**:992–998.
39. Keserü B, Barbosa-Sicard E, Schermuly RT, Tanaka H, Hammock BD, Weissmann N *et al*. Hypoxia-induced pulmonary hypertension: comparison of soluble epoxide hydrolase deletion vs. inhibition. *Cardiovasc Res* 2010;**85**:232–240.

SUPPLEMENTARY MATERIAL

Supplementary Results

Supplementary Figure 1

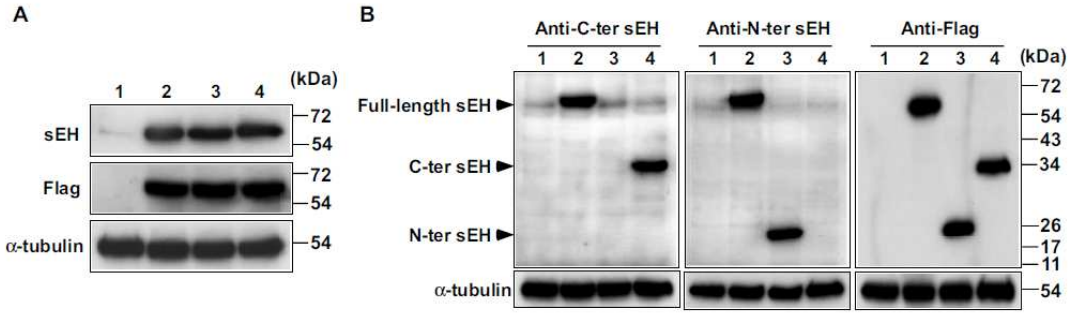

Supplementary Figure 1. Overexpression of full-length soluble epoxide hydrolase (sEH), N-terminal domain and C-terminal domain of sEH in bovine aortic endothelial cells (BAECs). (A) BAECs were transfected with Flag vector (lane 1), Flag-tag WT full-length sEH (lane 2), Flag-tag full-length sEH with phosphatase mutant (lane 3) or hydrolase mutant (lane 4) for 48 h. (B) BAECs were transfected with Flag vector (lane 1), Flag-tag full-length sEH (lane 2), Flag-tag N-terminal domain (N-ter sEH, lane 3) and C-terminal domain of sEH (C-ter sEH, lane 4) for 48 h. Cellular lysates were subjected to western blot analysis to examine the expression of full-length sEH, full-length sEH with phosphatase mutant, full-length sEH with hydrolase mutant, N-ter sEH or C-ter sEH by use of anti-Flag Ab, anti-C-ter sEH Ab or anti-N-ter sEH Ab. α-tubulin was used as the loading control.

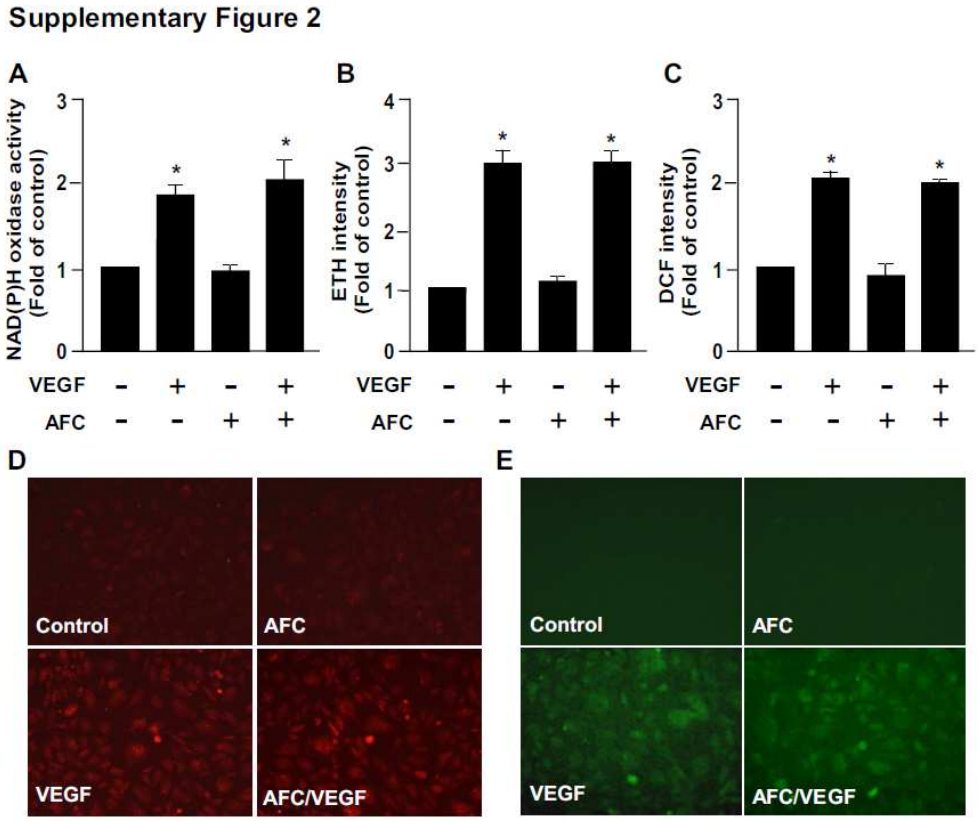

Supplementary Figure 2. Effect of phosphatase activity of soluble epoxide hydrolase (sEH) in vascular endothelial growth factor (VEGF)-induced increase in NAD(P)H oxidase activity and ROS production. Bovine aortic endothelial cells (BAECs) were pretreated with or without 50 μmol/L N-acetyl-S-farnesyl-L-cysteine (AFC, an inhibitor of phosphatase activity of sEH) for 2 h, then VEGF (50 ng/ml) for 30 min. The activity of NAD(P)H oxidase was examined by ELISA kit (A). Intracellular levels of $O_2^{\bullet -}$ and H_2O_2, respectively, were measured by use of HE/ethidium (B and D) and DCFH-DA/DCF (C and E) assays. $^{*}P < 0.05$ vs. vehicle-treated cells, $^{\#}P < 0.05$ vs. VEGF-treated alone cells.

Supplementary Figure 3

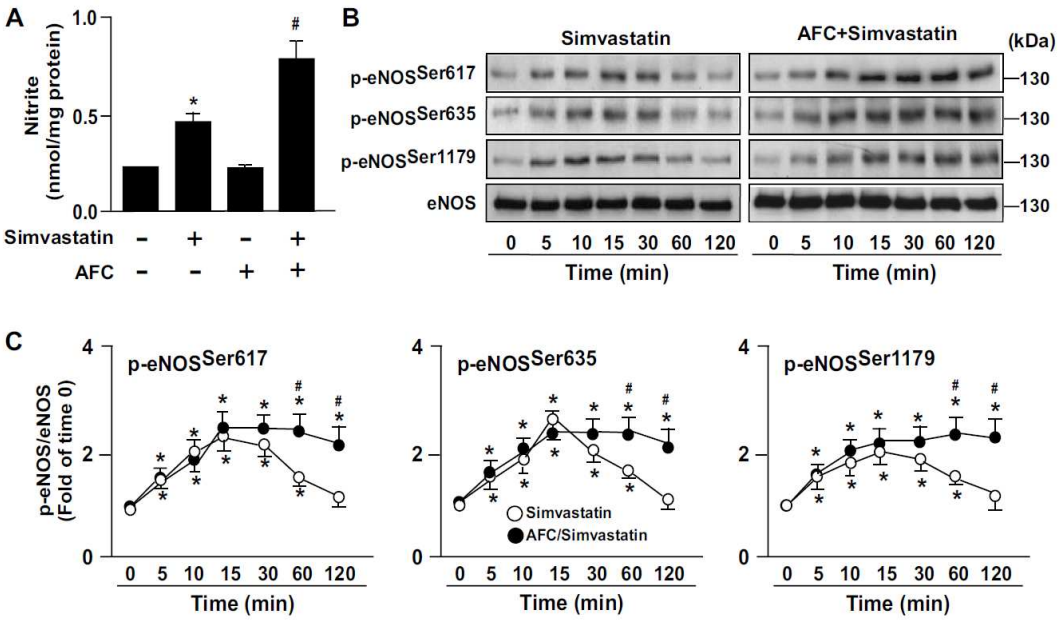

Supplementary Figure 3. Effect of phosphatase activity of soluble epoxide hydrolase (sEH) in simvastatin-induced NO production and eNOS phosphorylation. (A) Bovine aortic endothelial cells (BAECs) were pretreated with or without 50 μmol/L N-acetyl-S-farnesyl-L-cysteine (AFC, an inhibitor of phosphatase activity of sEH) for 2 h, then VEGF (50 ng/ml) for 24 h (A) or 0-120 min (B and C). Level of nitrite in culture media was measured by Griess assay. Cellular lysates were subjected to western blot analysis with Abs for phosphorylated eNOS (p-eNOS) at Ser617, Ser635 and Ser1179 and eNOS. $^{*}P < 0.05$ vs. vehicle-treated cells, $^{\#}P < 0.05$ vs. VEGF-treated alone cells.